Molecular fMRI

A Hai and A Jasanoff, Massachusetts Institute of Technology, Cambridge, MA, USA

Glossary

Blood–brain barrier (BBB) A system of tight junctions between endothelial cells and adhering astrocytes that prevents most blood-borne substances, including typical MRI contrast agents, from entering the brain.

Chemical exchange saturation transfer (CEST) agent An MRI contrast agent that acts via the CEST effect.

CEST effect A contrast mechanism that relies on the exchange of a spectrally resolved labile proton pool with bulk water protons. Saturating irradiation delivered at the nuclear magnetic resonance (NMR) frequency of the labile protons suppresses water proton signal at the bulk water frequency, due to chemical exchange between the two proton pools.

Heteronuclear agent An MRI molecular imaging probe that incorporates NMR-detectable atoms other than protons and can be imaged by dedicated MRI methods.

Hyperpolarization Any of several techniques for boosting the polarization of a spin population beyond the level normally achieved at thermal equilibrium in the field of an NMR or MRI instrument. Hyperpolarized substances can sometimes be detected with great sensitivity by MRI.

T_1 contrast agent An MRI contrast agent that accelerates longitudinal (T_1) relaxation and is conventionally visualized via signal enhancements in T_1-weighted scans.

T_2 contrast agent An MRI contrast agent that accelerates transverse (T_2) relaxation and is conventionally visualized via signal decreases in T_2-weighted scans.

Introduction

The realization that the dynamics of cerebral blood flow can be coupled to contrast in magnetic resonance imaging (MRI) scans opened the door to using MRI for the noninvasive imaging of neural activity-dependent blood flow changes in the brain (Belliveau et al., 1990, 1991; Ogawa, Lee, Kay, & Tank, 1990; Ogawa et al., 1992). This has transformed the fields of cognitive neuroscience and clinical neurology and has given rise to what are now the most prominent techniques to explore brain activation noninvasively, collectively known as functional magnetic resonance imaging (fMRI). Because conventional fMRI signals arise from cerebral hemodynamic processes, however, they provide only an indirect readout of neuronal activity (Logothetis & Wandell, 2004). Hemodynamic changes arise from a complex interplay of chemical signaling pathways that originate in both neurons and glia (Iadecola, 2004; Iadecola & Nedergaard, 2007). Hemodynamic signals therefore do not permit the discrimination of neural activity components associated with different cell types, neurotransmitters, or intracellular pathways; they also display nonlinear and sometimes sluggish dynamics with respect to neural signals.

In recent years, there have been growing attempts to combine MRI with molecular probes that allow monitoring of neurophysiological processes at molecular and cellular levels. Functional imaging with such probes ('molecular fMRI') can provide far greater specificity than hemodynamic imaging and also potentially superior spatial and temporal resolution. Molecular imaging with MRI is far less well developed as an approach, compared with optical imaging techniques or positron emission tomography (PET). In particular, MRI probes are less sensitively detected than either optical or PET probes (Weissleder & Pittet, 2008). Compared with optical imaging, however, molecular fMRI offers far greater spatial coverage and depth penetration into the tissue. Compared with PET molecular imaging (reviewed in this volume), MRI offers far better spatial and temporal resolution, as well as the possibility of dynamic sensing using MRI contrast agents that can be modulated by binding to target analytes in the brain. In the remainder of this article, we will introduce the basic mechanisms of molecular MRI agents and discuss how they may be applied for *in vivo* imaging of neurophysiological processes.

MRI Contrast Agents

The first MRI contrast agents were molecular compounds recognized for their ability to increase the nuclear magnetic relaxation rates of water molecules in the tissue. Because water proton density and relaxation are the primary determinants of conventional MRI signals, molecules that influence relaxation rates can modulate the MRI contrast by brightening or darkening portions of the imaged tissue (Merbach, Helm, & Toth, 2013). Such agents are now used in a wide variety of applications, including as blood pool agents for enhancing hemodynamic fMRI signals (Chen et al., 2001; Leite et al., 2002; Mandeville et al., 2001). More generally, molecular imaging agents for MRI can be divided into three main groups, according to the mechanisms by which they operate: (1) agents that increase the longitudinal (T_1) or transverse (T_2) spin relaxation rates, often termed T_1 or T_2 contrast agents; (2) agents that employ the chemical exchange saturation transfer (CEST) effect; and (3) 'heteronuclear' imaging agents that contain nuclei other than hydrogen (^{1}H), such as carbon (^{13}C) and fluorine (^{19}F), and can be detected using modified MRI equipment, but with a substantially lower signal due to their small quantity in the tissue. Different contrast agents that bind to or mimic compounds relevant to neurophysiology and brain activity and that employ these mechanisms are being continually developed and tested. We will discuss each mechanism and explore the main examples of its use for molecular brain fMRI.

T_1 and T_2 fMRI Probes

Typical MRI contrast is determined by proton density and by the so-called T_1 and T_2 relaxation times that reflect the dynamics of nuclear spin magnetization during an MRI scan. T_1 describes the characteristic time required for return to equilibrium magnetization after an MRI pulse sequence; T_1-weighted scans are brighter in areas of shorter T_1. T_2 describes the duration of MRI signal persistence after a pulse sequence; T_2-weighted scans are darker in areas of shorter T_2. Paramagnetic species shorten T_1 and T_2 relaxation times and can therefore act as contrast agents in T_1- and T_2-weighted scans (**Figure 1**). Contrast agents usually linearly increase $1/T_1$ (R_1) or $1/T_2$ (R_2) with constants of proportionality r_1 or r_2, respectively. Agents that exhibit $r_1 \sim r_2$ are referred to as T_1 agents and are observed primarily through T_1-weighted imaging; compounds that have $r_1 \ll r_2$ are referred to as T_2 agents and are usually observed using T_2-weighted MRI. Given typical relaxivities, most contrast agents must be applied at 10–100 μM concentrations to produce detectable effects on MRI contrast *in vivo*.

T_1 contrast agents usually contain paramagnetic metal ions bound to a chelator that reduces the inherent toxicity of metal ions in the tissue. Gadolinium (Gd^{3+}) ions are most frequently incorporated into T_1 contrast agents (Caravan, 2006), but manganese and iron ions are also increasingly used. T_2 contrast agents usually contain crystalline metal compounds such as particles of iron oxide ranging from several nanometers to hundreds of nanometers in diameter (Vogl et al., 1996). Such nanoparticles exhibit cooperative magnetic behavior and are termed superparamagnetic; microscopic magnetic fields produced by superparamagnetic particles in an MRI scanner are particularly potent sources of T_2 relaxation.

For T_1 or T_2 agents to be used in functional imaging of the brain, modulation of their contrast effects must be coupled to neural activity in some way. One of the first successful attempts at developing contrast agents that are coupled to neural activity made use of the paramagnetic divalent ion manganese (Mn^{2+}) as a tracer for monitoring neuronal calcium (Ca^{2+}) ions (Lin & Koretsky, 1997). Calcium ions participate in neural signaling events such as synaptic activity, neurotransmitter release, and

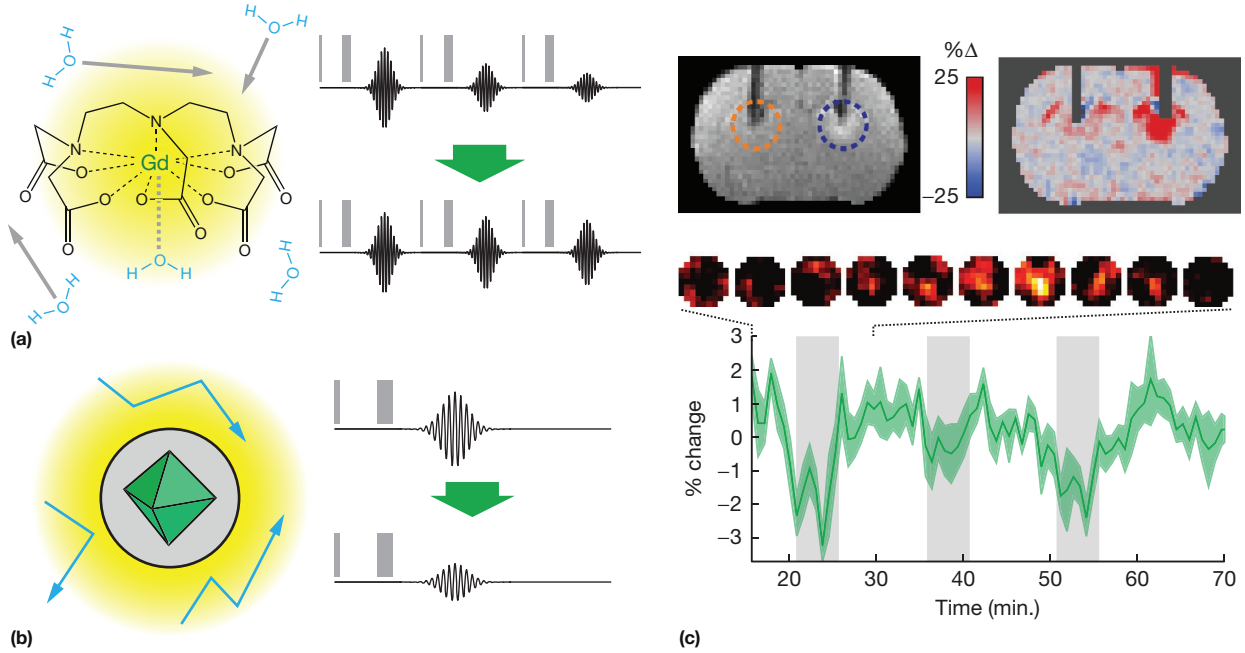

Figure 1 T_1 and T_2 contrast agents for molecular (functional magnetic resonance imaging) fMRI. (a) T_1 contrast agents most commonly consist of paramagnetic atoms such as gadolinium, manganese, or iron, bound to a chelate. A canonical example, Gd^{3+}–diethylenetriaminepentaacetic acid, is shown at the left. Such contrast agents interact with water molecules (blue) either directly (dotted line) or through space to promote changes in water proton T_1 magnetic relaxation rate. A shortened T_1 results in better recovery of the (magnetic resonance imaging) MRI signal (black traces at the right) between repetitions of the pulse sequence (gray bars), thereby increasing the observed image intensity. (b) T_2 agents, usually in the form of polymer-coated superparamagnetic nanoparticles (green), induce magnetic field inhomogeneities (yellow) that promote relaxation of nearby diffusing water protons (blue arrows) and a reduction of the MRI signal observed after each repetition of the pulse sequence (right panel). (c) A protein-based contrast agent derived from the heme domain of the bacterial cytochrome P450-BM3 binds the neurotransmitter dopamine with an ~80% change in T_1 relaxivity *in vivo* (Shapiro et al., 2010). Shown in the upper left panel is a coronal slice of a rat brain injected with the dopamine-sensing agent with (orange circle) and without (blue circle) equimolar dopamine. The upper right panel shows color-coded signal change through the injection of the agent; because the contrast agent turns off in the presence of dopamine, the coinjection region shows little signal change while the sensor-only region shows a 25% signal increase. The bottom panel shows a molecular fMRI measurement made using the sensor during three pulses of potassium stimulation (gray bars) in intracranially injected rat striatum. The snapshots above show signal variation in the injected region over one stimulus cycle. The green trace shows the time course of significantly modulated voxels in the images. Reprinted from Jasanoff, A. (2007). MRI contrast agents for functional molecular imaging of brain activity. *Current Opinion in Neurobiology*, *17*, 593–600, with permission from Elsevier, Copyright (2007).

electric signaling in the form of dendritic spikes, and their abundance in neural tissue poses an advantage for a mimetic contrast agent. Manganese can enter the cell using the same voltage-gated Ca^{2+} channels through which calcium ions pass (Meiri & Rahamimo, 1972; Narita, Kawasaki, & Kita, 1990). These data show that manganese accumulates in active cells and slowly washes out (on the order of days) and thus acts as a T_1-weighted MRI label for neural activity (Lin & Koretsky, 1997) and an agent for enhancing contrast dependent on neural architecture in the brain (Aoki, Wu, Silva, Lynch, & Koretsky, 2004; Pautler, Silva, & Koretsky, 1998; Silva et al., 2008). Further efforts to create calcium-sensitive T_1 contrast agents made use of the calcium chelators 1,2-bis-(*O*-aminophenoxy) ethane-*N*,*N*,*N*′,*N*′-tetraacetic acid (BAPTA) (Li, Fraser, & Meade, 1999) and ethylene glycol tetraacetic acid (Angelovski et al., 2008) covalently conjugated to derivatives of the paramagnetic gadolinium (Gd^{3+})-1,4,7,10-tetraazacyclododecane-1,4,7,10-tetraacetic acid (Gd-DOTA) complex. These agents show changes in relaxivity in response to physiologically relevant Ca^{2+} concentrations *in vitro*.

Other endogenous metal ions such as copper and zinc also influence neural function and processes of neuropathology (Que, Domaille, & Chang, 2008), albeit not as ubiquitously as calcium. In particular, mobile zinc ions are coreleased with glutamate in some brain regions and may play a part in regulating synaptic plasticity. Zinc-binding contrast agents have been formed by combining paramagnetic chelating moieties with zinc-binding motifs such as *N*,*N*,*N*′,*N*′-tetrakis(2-pyridylmethyl)ethylenediamine (Hanaoka et al., 2002), dipicolylamine (DPA) (Esqueda et al., 2009; Zhang, Lovejoy, Jasanoff, & Lippard, 2007), and 2,2′-azanediyldiacetate (Major, Parigi, Luchinat, & Meade, 2007). Gadolinium-based zinc sensors derived from these platforms have been shown to undergo two- to threefold changes in r_1 and to allow *in vitro* detection of physiologically relevant Zn^{2+} concentrations as low as 30 μM. A manganese porphyrin-DPA conjugate displays more modest zinc-dependent r_1 changes (Zhang et al., 2007) but was shown to undergo Zn^{2+}-dependent uptake by cells and to provide preferential contrast enhancement of hippocampal neurons *in vivo* (Lee et al., 2010), possibly reflecting enhanced zinc content of these cells. A Gd^{3+} chelator fused to a copper recognition motif has been demonstrated to respond to copper by modulating its T_1 relaxivity *in vitro* (Que & Chang, 2006). Disrupted copper homeostasis is associated with Alzheimer's disease and amyloid accumulation (Squitti & Polimanti, 2013), though a role for copper in normal neural signaling processes has not been established.

Combining superparamagnetic iron oxide (SPIO) nanoparticles with neurophysiologically relevant sensing domains can actuate T_2 relaxivity changes suitable for functional imaging. A prominent application of this principle to calcium sensing made use of two groups of SPIO nanoparticles conjugated to the calcium-sensing protein calmodulin (CaM) and to a Ca_4CaM-binding peptide (RS20) (Atanasijevic, Shusteff, Fam, & Jasanoff, 2006). In the presence of calcium, the CaM and RS20-functionalized SPIO nanoparticles interact and cause aggregation of the particles and a change in T_2 relaxivity with a calcium sensitivity of ~1 μM *in vitro*. Another example of iron oxide-based T_2 contrast agent uses intraventricularly injected microscale iron oxide particles, which are spontaneously taken up by neural progenitor cells in the brain *in vivo* (Sumner, Shapiro, Maric, Conroy, & Koretsky, 2009). Although this technique does not allow monitoring of neural signaling per se, it was shown to allow tracking of migrating cells that participate in the maintenance and plasticity of neural circuitry in the forebrain.

More recent efforts make use of protein-based contrast agents, which can act as genetically encoded MRI sensors suitable for biosynthesis or expression in genetically modified subjects (Matsumoto & Jasanoff, 2013). One family of protein molecular imaging agents was formed using directed *in vitro* evolution of an iron-containing protein, derived from the heme domain of the bacterial cytochrome P450-BM3, to bind the neurotransmitters dopamine (Shapiro et al., 2010) and serotonin (Brustad et al., 2012). In the resulting probes, dopamine binding to a site near the protein's paramagnetic heme iron results in a drop in MRI signal due to reduced access of water protons to the iron and reduced T_1 relaxivity in the presence of the dopamine at concentrations of several micromolar. This dopamine sensor was shown to detect neural activity elicited by potassium stimulation in live rat brains (**Figure 1(c)**). Another series of studies demonstrated that a genetically expressed nanoparticle contrast agent formed from the iron storage protein ferritin could act as an endogenously expressed contrast agent in virally transduced (Genove, DeMarco, Xu, Goins, & Ahrens, 2005) or transgenic (Cohen, Dafni, Meir, Harmelin, & Neeman, 2005) animals. A sensor for neuronal kinase activity was constructed from genetically engineered ferritins (Shapiro, Szablowski, Langer, & Jasanoff, 2009) and characterized *in vitro*, suggesting long-term prospects for engineering functional imaging reporters from these species. Additional MRI gene reporting strategies have been proposed based on paramagnetic metal transporters (Gruppi et al., 2012; Zurkiya, Chan, & Hu, 2008) or by combining the expression of a reporter enzyme with a synthetic MRI contrast agent substrate (Hsieh & Jasanoff, 2012). One of the earliest such attempts combined the expression of the well-known β-galactosidase enzyme with a responsive T_1 contrast agent that enabled reporter detection in frog embryos (Louie et al., 2000).

CEST Agents

A different group of MRI contrast agents makes use of compounds that can exchange protons with surrounding water molecules in what is termed proton CEST (Ward, Aletras, & Balaban, 2000). In this modality, chemicals containing exchangeable protons with resonance frequencies that are well resolved from protons in bulk water are imaged using a specialized MRI pulse sequence (**Figure 2**). In the CEST pulse sequence, strong 'saturating' radiofrequency irradiation is delivered at the resonance frequency of the exchanging protons; this suppresses their magnetization and detectability by MRI. Because the saturated protons are in exchange with water protons that give rise to most of the MRI contrast, the overall MRI signal in proximity to the CEST agent is also reduced. The proton exchange rate, frequency offset between bound and bulk water protons, intensity of saturation irradiation, and relaxation rates all combine to determine the magnitude of resulting CEST contrast (Woessner, Zhang, Merritt, & Sherry, 2005; Zhou, Wilson, Sun, Klaus, &

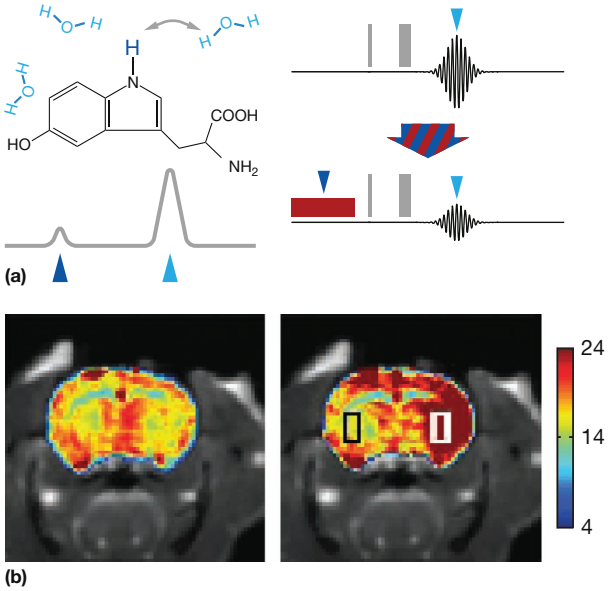

Figure 2 Chemical exchange saturation transfer (CEST) agents are chemicals that contain exchangeable protons with resonance frequencies that are well resolved from protons in bulk water. (a) An example shown is the indole nitrogen proton (indigo) of 5-hydroxytryptophan. The nuclear magnetic resonance spectrum of this compound in solution is schematized by the gray trace at the bottom left, where resonances of the CEST agent protons and water protons are indicated by indigo and cyan arrowheads, respectively. The right panel shows the CEST pulse sequence, in which strong 'saturating' radiofrequency irradiation (red) is delivered at the resonance frequency of the exchanging protons. Because the saturated protons are in exchange with water protons that give rise to most of the MRI contrast, the overall MRI signal due to water protons in proximity to the CEST agent is also reduced (cyan arrowheads). (b) The CEST effect can be used to detect proton transfer between the amine group of the ubiquitous neurotransmitter glutamate and nearby water molecules (Cai et al., 2012). This work demonstrated that cerebral artery occlusion stroke in rat brain generates a detectable increase of the glutamate CEST signal. Shown are maps acquired 1 h (left) and 4.5 h (right) after the induction of stroke. Areas ipsilateral and contralateral to the stroke are indicated by white and black rectangles, respectively. The color scale indicates the magnitude of contrast due to CEST probe-specific radiofrequency saturation, with respect to control irradiation. Reprinted from Cai, K. J., et al., (2012). Magnetic resonance imaging of glutamate. *Nature Medicine*, *18*, 302–306, with permission from Macmillan Publishers Ltd, Copyright 2012.

van Zijl, 2004). Because the selectivity with which CEST effects can be experimentally manipulated using the MRI pulse sequence, CEST contrast can be switched on and off. On the other hand, CEST contrast is typically weaker than relaxation-based MRI contrast, and millimolar concentrations of exchangeable protons are typically required to produce observable effects.

CEST contrast and CEST agents have been applied to detect a variety of phenomena relevant to functional brain imaging. Subtle changes in brain pH are associated with neural activity (Chesler, 2003), and because pH changes relate closely to proton exchange, they are therefore particularly suitable for detection by CEST agents. CEST contrast arising from saturation of intrinsic exchanging amide protons has been used to measure pH *in vivo*, and pH changes of roughly 0.5 units associated with ischemic stroke in rat brains could be imaged (Zhou, Payen, Wilson, Traystman, & van Zijl, 2003). Sensitivity of this method or of related T_1 contrast-based molecular imaging approaches (Raghunand, Zhang, Sherry, & Gillies, 2002) would need to be improved in order to detect normal brain activity via pH.

An effort to detect gene expression by CEST made use of a genetically expressed lysine-rich protein (LRP) reporter of which the proton exchange between its amide protons and water molecules is detected by CEST MRI in rat brains (Gilad et al., 2007). Although the signal changes produced by the LRP were small and required long imaging time (>30 min), they are potentially less prone to artifacts than MRI changes reported by relaxation-based agents such as ferritin, and they do not require slow and potentially toxic accumulation of metal ions. Another recent CEST approach enabled specific detection of proton transfer between the amine group of the ubiquitous neurotransmitter glutamate and water molecules (Cai et al., 2012). This work demonstrated that cerebral artery occlusion in rat brain generates a 100% increase of the glutamate CEST signal in the appropriate frequency shift (**Figure 2(b)**). In addition, the authors showed increase in CEST signal upon intravenous injection of glutamate in a tumor model with blood–brain barrier (BBB) disruption. Although these experiments demonstrated molecular MRI of glutamate in rat brain under extreme physiological conditions, a follow-up study (Cai et al., 2013) also showed the ability of the technique to generate a static map of glutamate in healthy human brains similar to PET studies (Ametamey et al., 2007), but without the need for exogenous agents.

Molecular imaging using CEST MRI in the brain suffers from signal reduction due to the magnetization transfer effect from other endogenous molecules. A variation of CEST MRI termed PARACEST uses paramagnetic lanthanides for significantly higher concentration delectability, in the nanomolar range (Zhang, Merritt, Woessner, Lenkinski, & Sherry, 2003). Initial attempts to use a lanthanide-based agent in the form of a thulium (Tm^{3+}) chelate bound to the ligand DOTAM-glycine-lysine for brain imaging show uptake of the agent in mouse brain tumor assay (Li et al., 2011). Although this study has not shown sensitivity in the nanomolar range, it nonetheless opens the possibility for a more sensitive family of contrast agents for brain MRI.

Heteronuclear Probes

Molecular imaging agents containing nuclei other than protons, such as carbon (^{13}C) and fluorine (^{19}F), may be imaged using modified MRI hardware specifically tuned to the resonance frequencies of these nuclei. The MRI signal arising from such 'heteronuclear probes' is considerably weaker than that of endogenous water protons because of the much lower abundance of heteronuclear species, compounded by the intrinsically lower sensitivity of MRI techniques to nuclei other than hydrogen. A long history of magnetic resonance spectroscopy and spectroscopic imaging has enabled the detection of ^{13}C-containing metabolites related to brain function. Using these approaches, it has been possible to perform functional studies that detect the effect of neural activity on glutamate metabolism (Rothman et al., 1992; Sibson et al., 1997), albeit

with low temporal resolution due to the insensitivity of MRI to endogenous ^{13}C. A strategy for breaking past this sensitivity limit makes use of a technique called dynamic nuclear polarization (DNP) to enhance the polarization, and hence the detectability, of ^{13}C species beyond what can be achieved using conventional MRI (Ardenkjaer-Larsen et al., 2003; Golman, in't Zandt, & Thaning, 2006). DNP and related hyperpolarization techniques are implemented outside the MRI scanner, and hyperpolarized substances are then injected and imaged in the subject. Because polarization decays back to thermal equilibrium levels by T_1 relaxation processes, manipulation and imaging using hyperpolarized agents must be performed rapidly, within a few minutes for ^{13}C. In the work of Golman et al. (2006), ^{13}C-labeled pyruvate was hyperpolarized and injected *in vivo*. Using spectroscopic MRI techniques, the study demonstrates simultaneous maps of pyruvate, lactate, and alanine with millimeter spatial resolution, enabling measurements of metabolic turnover rates over tens of seconds. Similar approaches, perhaps in conjunction with efforts to polarize substances more specifically related to neurochemistry (Allouche-Arnon, Lerche, Karlsson, Lenkinski, & Katz-Brull, 2011; Allouche-Arnon et al., 2011), may eventually prove useful for molecular fMRI in the nervous system. An additional possible avenue involves the use of silicon nanoparticles as hyperpolarizable contrast agents; these nanoparticles display relaxation times on the order of minutes to hours and at room temperature (Aptekar et al., 2009), allowing imaging to take place over a much longer period of time than with ^{13}C-labeled agents. This advantage, together with the ability to easily functionalize silicon with biologically relevant molecules, allows for a myriad of potential applications.

Efforts to image ^{19}F-labeled compounds benefit from the low background of ^{19}F in biological subjects and the relative sensitivity with which fluorinated compounds can be detected by MRI, ~90% that of protons, even without hyperpolarization. Imaging of ^{19}F-labeled amyloidophilic compounds can be used for the *in vivo* detection of amyloid beta plaques in mouse models of Alzheimer's disease with submillimeter resolution and imaging times of a couple of hours (Higuchi et al., 2005). Another ^{19}F imaging study makes use of a Gd–peptide–^{19}F complex whereby the ^{19}F MRI signal is attenuated by an intramolecular Gd^{3+} chelate moiety and is modulated by the activity of proteases that cleave the probe (Mizukami et al., 2008). Both of these studies open the door for functional imaging of neuropathologic pathways using fluorinated probes. An additional and recent study combining heteronuclear imaging of ^{19}F with CEST exploits the chemical shift change of a 5,5′-difluoro derivative of BAPTA upon binding to Ca^{2+} ions for the detection of Ca^{2+} concentrations as low as 0.5 μM (Bar-Shir et al., 2013). Combining ^{19}F MRI detection with high spatial and temporal resolution is challenging, but functional measurements may still be possible in cases where appropriate trade-offs can be made.

Challenges for Molecular fMRI of the Brain

The delivery of contrast agents into the brain is problematic due to the existence of the blood–brain barrier. This system of tight junctions between the vascular endothelial cells and adhering astrocytes not only prevents potentially harmful substances in the bloodstream from entering the brain but also blocks therapeutics and imaging agents. Strategies to transiently disrupt the BBB include the administration of a hyperosmotic shock by intravascular injection of a hypertonic substance such as 25% mannitol (Neuwelt & Rapoport, 1984) and more recently by the application of focused or unfocused ultrasound, in which the BBB is disrupted by sonic pressure waves amplified by intravascular gas-filled microbubbles (Vykhodtseva, McDannold, & Hynynen, 2008). Both osmotic shock and ultrasound methods have been used to deliver T_1 and T_2 agents in sufficient quantities for MRI observation. Other trans-BBB delivery methods use endogenous transport mechanisms involving transferrin and insulin receptors (Pardridge, 2012) and cell-penetrating peptides (Santra et al., 2004) to deliver agents across the BBB, but these may not be effective enough for the delivery of MRI contrast agents at useful doses.

The requirement for exogenous delivery of contrast agents is a substantial drawback of many molecular fMRI approaches, compared with hemodynamic fMRI. A significant advantage of molecular techniques is that they can in principle achieve much higher spatial and temporal resolution, however, because they are not limited by the spatiotemporal properties of blood flow changes. The ultimate spatial resolution of MRI is usually placed in the 1–10 μm range, limited by the diffusion of water molecules in the tissue; in practice, this resolution is rarely achieved, however, because of the long measuring times required for the buildup of adequate signal-to-noise ratio, particularly *in vivo*. Current molecular MRI techniques can provide spatial resolution on the order of 100 μm and temporal resolution on the order of seconds, but with trade-offs between the two. Substantial efforts are needed to move toward millisecond timescales and micrometer spatial features most relevant to neuronal activity and structure. Gains are most likely to be made by improving the potency of MRI contrast agents, going to higher MRI magnetic fields, and optimizing pulse sequences for molecular applications. Molecular fMRI techniques are still in their infancy, but offer one of few paths toward truly noninvasive whole-brain analysis of neural activity at molecular and cellular levels, particularly if technological developments continue along their present course.

See also: **INTRODUCTION TO ACQUISITION METHODS**: Contrast Agents in Functional Magnetic Resonance Imaging; Obtaining Quantitative Information from fMRI; PET; Optical imaging.

References

Allouche-Arnon, H., Lerche, M. H., Karlsson, M., Lenkinski, R. E., & Katz-Brull, R. (2011). Deuteration of a molecular probe for DNP hyperpolarization – A new approach and validation for choline chloride. *Contrast Media & Molecular Imaging*, *6*, 499–506.

Allouche-Arnon, H., et al. (2011). A hyperpolarized choline molecular probe for monitoring acetylcholine synthesis. *Contrast Media & Molecular Imaging*, *6*, 139–147.

Ametamey, S. M., et al. (2007). Human PET studies of metabotropic glutamate receptor subtype 5 with C-11-ABP688. *Journal of Nuclear Medicine*, *48*, 247–252.

Angelovski, G., Fouskova, P., Mamedov, I., Canals, S., Toth, E., & Logothetis, N. K. (2008). Smart magnetic resonance imaging agents that sense extracellular calcium fluctuations. *Chembiochem*, *9*, 1729–1734.

Aoki, I., Wu, Y. J.L, Silva, A. C., Lynch, R. M., & Koretsky, A. P. (2004). In vivo detection of neuroarchitecture in the rodent brain using manganese-enhanced MRI. *NeuroImage*, *22*, 1046–1059.

Aptekar, J. W., et al. (2009). Silicon nanoparticles as hyperpolarized magnetic resonance imaging agents. *ACS Nano*, *3*, 4003–4008.

Ardenkjaer-Larsen, J. H., et al. (2003). Increase in signal-to-noise ratio of >10,000 times in liquid-state NMR. *Proceedings of the National Academy of Sciences of the United States of America*, *100*, 10158–10163.

Atanasijevic, T., Shusteff, M., Fam, P., & Jasanoff, A. (2006). Calcium-sensitive MRI contrast agents based on superparamagnetic iron oxide nanoparticles and calmodulin. *Proceedings of the National Academy of Sciences of the United States of America*, *103*, 14707–14712.

Bar-Shir, A., et al. (2013). Metal ion sensing using ion chemical exchange saturation transfer (19)F magnetic resonance imaging. *Journal of the American Chemical Society*, *135*, 12164–12167.

Belliveau, J. W., et al. (1990). Functional cerebral imaging by susceptibility-contrast NMR. *Magnetic Resonance in Medicine*, *14*, 538–546.

Belliveau, J. W., et al. (1991). Functional mapping of the human visual-cortex by magnetic-resonance-imaging. *Science*, *254*, 716–719.

Brustad, E. M., et al. (2012). Structure-guided directed evolution of highly selective p450-based magnetic resonance imaging sensors for dopamine and serotonin. *Journal of Molecular Biology*, *422*, 245–262.

Cai, K. J., et al. (2012). Magnetic resonance imaging of glutamate. *Nature Medicine*, *18*, 302–306.

Cai, K., et al. (2013). Mapping glutamate in subcortical brain structures using high-resolution GluCEST MRI *NMR in Biomedicine*, .

Caravan, P. (2006). Strategies for increasing the sensitivity of gadolinium based MRI contrast agents. *Chemical Society Reviews*, *35*, 512–523.

Chen, Y. C.I, Mandeville, J. B., Nguyen, T. V., Talele, A., Cavagna, F., & Jenkins, B. G. (2001). Improved mapping of pharmacologically induced neuronal activation using the IRON technique with superparamagnetic blood pool agents. *Journal of Magnetic Resonance Imaging*, *14*, 517–524.

Chesler, M. (2003). Regulation and modulation of pH in the brain. *Physiological Reviews*, *83*, 1183–1221.

Cohen, B., Dafni, H., Meir, G., Harmelin, A., & Neeman, M. (2005). Ferritin as an endogenous MRI reporter for noninvasive imaging of gene expression in C6 glioma tumors. *Neoplasia*, *7*, 109–117.

Esqueda, A. C., et al. (2009). A new gadolinium-based MRI zinc sensor. *Journal of the American Chemical Society*, *131*, 11387–11391.

Genove, G., DeMarco, U., Xu, H. Y., Goins, W. F., & Ahrens, E. T. (2005). A new transgene reporter for in vivo magnetic resonance imaging. *Nature Medicine*, *11*, 450–454.

Gilad, A. A., et al. (2007). Artificial reporter gene providing MRI contrast based on proton exchange. *Nature Biotechnology*, *25*, 217–219.

Golman, K., in't Zandt, R., & Thaning, M. (2006). Real-time metabolic imaging. *Proceedings of the National Academy of Sciences of the United States of America*, *103*, 11270–11275.

Gruppi, F., Liang, J., Bartelle, B. B., Royzen, M., Turnbull, D. H., & Canary, J. W. (2012). Supramolecular metal displacement allows on-fluorescence analysis of manganese (II) in living cells. *Chemical Communications*, *48*, 10778–10780.

Hanaoka, K., et al. (2002). Design and synthesis of a novel magnetic resonance imaging contrast agent for selective sensing of zinc ion. *Chemistry & Biology*, *9*, 1027–1032.

Higuchi, M., Iwata, N., Matsuba, Y., Sato, K., Sasamoto, K., & Saido, T. C. (2005). F-19 and H-1 MRI detection of amyloid beta plaques in vivo. *Nature Neuroscience*, *8*, 527–533.

Hsieh, V., & Jasanoff, A. (2012). Bioengineered probes for molecular magnetic resonance imaging in the nervous system. *ACS Chemical Neuroscience*, *3*, 593–602.

Iadecola, C. (2004). Neurovascular regulation in the normal brain and in Alzheimer's disease. *Nature Reviews. Neuroscience*, *5*, 347–360.

Iadecola, C., & Nedergaard, M. (2007). Glial regulation of the cerebral microvasculature. *Nature Neuroscience*, *10*, 1369–1376.

Lee, T., Zhang, X.-A., Dhar, S., Faas, H., Lippard, S. J., & Jasanoff, A. (2010). In vivo imaging with a cell-permeable porphyrin-based MRI contrast agent. *Chemistry & Biology*, *17*, 665–673.

Leite, F. P., et al. (2002). Repeated fMRI using iron oxide contrast agent in awake, behaving macaques at 3 Tesla. *NeuroImage*, *16*, 283–294.

Li, W. H., Fraser, S. E., & Meade, T. J. (1999). A calcium-sensitive magnetic resonance imaging contrast agent. *Journal of the American Chemical Society*, *121*, 1413–1414.

Li, A. X., et al. (2011). In vivo detection of MRI-PARACEST agents in mouse brain tumors at 9.4 T. *Magnetic Resonance in Medicine*, *66*, 67–72.

Lin, Y. J., & Koretsky, A. P. (1997). Manganese ion enhances T-1-weighted MRI during brain activation: An approach to direct imaging of brain function. *Magnetic Resonance in Medicine*, *38*, 378–388.

Logothetis, N. K., & Wandell, B. A. (2004). Interpreting the BOLD signal. *Annual Review of Physiology*, *66*, 735–769.

Louie, A. Y., et al. (2000). In vivo visualization of gene expression using magnetic resonance imaging. *Nature Biotechnology*, *18*, 321–325.

Major, J. L., Parigi, G., Luchinat, C., & Meade, T. J. (2007). The synthesis and in vitro testing of a zinc-activated MRI contrast agent. *Proceedings of the National Academy of Sciences of the United States of America*, *104*, 13881–13886.

Mandeville, J. B., Jenkins, B. G., Kosofsky, B. E., Moskowitz, M. A., Rosen, B. R., & Marota, J. J.A (2001). Regional sensitivity and coupling of BOLD and CBV changes during stimulation of rat brain. *Magnetic Resonance in Medicine*, *45*, 443–447.

Matsumoto, Y., & Jasanoff, A. (2013). Metalloprotein-based MRI probes. *FEBS Letters*, *587*, 1021–1029.

Meiri, U., & Rahamimo, R. (1972). Neuromuscular transmission – Inhibition by manganese ions. *Science*, *176*, 308–309.

Merbach, A. S., Helm, L., & Toth, E. (2013). *The chemistry of contrast agents in medical magnetic resonance imaging*. Chichester, UK: Wiley.

Mizukami, S., et al. (2008). Paramagnetic relaxation-based F-19 MRI probe to detect protease activity. *Journal of the American Chemical Society*, *130*, 794–795.

Narita, K., Kawasaki, F., & Kita, H. (1990). Mn and Mg influxes through Ca channels of motor-nerve terminals are prevented by verapamil in frogs. *Brain Research*, *510*, 289–295.

Neuwelt, E. A., & Rapoport, S. I. (1984). Modification of the blood–brain-barrier in the chemotherapy of malignant brain-tumors. *Federation Proceedings*, *43*, 214–219.

Ogawa, S., Lee, T. M., Kay, A. R., & Tank, D. W. (1990). Brain magnetic-resonance-imaging with contrast dependent on blood oxygenation. *Proceedings of the National Academy of Sciences of the United States of America*, *87*, 9868–9872.

Ogawa, S., et al. (1992). Intrinsic signal changes accompanying sensory stimulation – Functional brain mapping with magnetic-resonance-imaging. *Proceedings of the National Academy of Sciences of the United States of America*, *89*, 5951–5955.

Pardridge, W. M. (2012). Drug transport across the blood–brain barrier. *Journal of Cerebral Blood Flow and Metabolism*, *32*, 1959–1972.

Pautler, R. G., Silva, A. C., & Koretsky, A. P. (1998). In vivo neuronal tract tracing using manganese-enhanced magnetic resonance imaging. *Magnetic Resonance in Medicine*, *40*, 740–748.

Que, E. L., & Chang, C. J. (2006). A smart magnetic resonance contrast agent for selective copper sensing. *Journal of the American Chemical Society*, *128*, 15942–15943.

Que, E. L., Domaille, D. W., & Chang, C. J. (2008). Metals in neurobiology: Probing their chemistry and biology with molecular imaging. *Chemical Reviews*, *108*, 1517–1549.

Raghunand, N., Zhang, S. R., Sherry, A. D., & Gillies, R. J. (2002). In vivo magnetic resonance imaging of tissue pH using a novel pH-sensitive contrast agent, GdDOTA-4AmP. *Academic Radiology*, *9*, S481–S483.

Rothman, D. L., et al. (1992). H-1 C-13 NMR measurements of 4-C-13 glutamate turnover in human brain. *Proceedings of the National Academy of Sciences of the United States of America*, *89*, 9603–9606.

Santra, S., et al. (2004). TAT conjugated, FITC doped silica nanoparticles for bioimaging applications. *Chemical Communications*, 2810–2811.

Shapiro, M. G., Szablowski, J. O., Langer, R., & Jasanoff, A. (2009). Protein nanoparticles engineered to sense kinase activity in MRI. *Journal of the American Chemical Society*, *131*, 2484–2486.

Shapiro, M. G., et al. (2010). Directed evolution of a magnetic resonance imaging contrast agent for noninvasive imaging of dopamine. *Nature Biotechnology*, *28*, 264–270.

Sibson, N. R., Dhankhar, A., Mason, G. F., Behar, K. L., Rothman, D. L., & Shulman, R. G. (1997). In vivo C-13 NMR measurements of cerebral glutamine synthesis as evidence for glutamate-glutamine cycling. *Proceedings of the National Academy of Sciences of the United States of America*, *94*, 2699–2704.

Silva, A. C., et al. (2008). Detection of cortical laminar architecture using manganese-enhanced MRI. *Journal of Neuroscience Methods*, *167*, 246–257.

Squitti, R., & Polimanti, R. (2013). Copper phenotype in Alzheimer's disease: Dissecting the pathway. *American Journal of Neurodegenerative Disease*, *2*, 46–56.

Sumner, J. P., Shapiro, E. M., Maric, D., Conroy, R., & Koretsky, A. P. (2009). In vivo labeling of adult neural progenitors for MRI with micron sized particles of iron oxide: Quantification of labeled cell phenotype. *NeuroImage*, *44*, 671–678.

Vogl, T. J., et al. (1996). Superparamagnetic iron oxide-enhanced versus gadolinium-enhanced MR imaging for differential diagnosis of focal liver lesions. *Radiology*, *198*, 881–887.

Vykhodtseva, N., McDannold, N., & Hynynen, K. (2008). Progress and problems in the application of focused ultrasound for blood–brain barrier disruption. *Ultrasonics*, *48*, 279–296.

Ward, K. M., Aletras, A. H., & Balaban, R. S. (2000). A new class of contrast agents for MRI based on proton chemical exchange dependent saturation transfer (CEST). *Journal of Magnetic Resonance*, *143*, 79–87.

Weissleder, R., & Pittet, M. J. (2008). Imaging in the era of molecular oncology. *Nature*, *452*, 580–589.

Woessner, D. E., Zhang, S. R., Merritt, M. E., & Sherry, A. D. (2005). Numerical solution of the Bloch equations provides insights into the optimum design of PARACEST agents for MRI. *Magnetic Resonance in Medicine*, *53*, 790–799.

Zhang, X. A., Lovejoy, K. S., Jasanoff, A., & Lippard, S. J. (2007). Water-soluble porphyrins imaging platform for MM zinc sensing. *Proceedings of the National Academy of Sciences of the United States of America*, *104*, 10780–10785.

Zhang, S. R., Merritt, M., Woessner, D. E., Lenkinski, R. E., & Sherry, A. D. (2003). PARACEST agents: Modulating MRI contrast via water proton exchange. *Accounts of Chemical Research*, *36*, 783–790.

Zhou, J. Y., Payen, J. F., Wilson, D. A., Traystman, R. J., & van Zijl, P. C. M. (2003). Using the amide proton signals of intracellular proteins and peptides to detect pH effects in MRI. *Nature Medicine*, *9*, 1085–1090.

Zhou, J. Y., Wilson, D. A., Sun, P. Z., Klaus, J. A., & van Zijl, P. C. M. (2004). Quantitative description of proton exchange processes between water and endogenous and exogenous agents for WEX, CEST, and APT experiments. *Magnetic Resonance in Medicine*, *51*, 945–952.

Zurkiya, O., Chan, A. W.S, & Hu, X. (2008). MagA is sufficient for producing magnetic nanoparticles in mammalian cells, making it an MRI reporter. *Magnetic Resonance in Medicine*, *59*, 1225–1231.